

# A supply-limited torrent that does not feel the heat of climate change

Received: 21 November 2023

Accepted: 9 October 2024

Published online: 21 October 2024

 Check for updates

Jiazhi Qie <sup>1</sup>✉, Adrien Favillier <sup>1,2</sup>, Frédéric Liébault <sup>3</sup>,  
Juan Antonio Ballesteros Cánovas <sup>1,4</sup>, Jérôme Lopez-Saez<sup>1</sup>, Sébastien Guillet <sup>1</sup>,  
Loïc Francon<sup>1</sup>, Yihua Zhong<sup>1</sup>, Markus Stoffel <sup>1,2,5</sup>✉ & Christophe Corona <sup>1,6</sup>

Debris-flow activity in the Alps is anticipated to undergo pronounced changes in response to a warming climate. Yet, a fundamental challenge in comprehensively assessing changes in process activity is the systematic lack of long-term observational debris-flow records. Here, we reconstruct the longest, continuous time series (1626–2020) of debris flows at Multetta, a supply-limited torrential system in the Eastern Swiss Alps. Relying on growth-ring records of trees that were damaged by debris flows, we do not detect significant changes in the frequency or magnitude over time. This seeming absence of a direct climatic influence on debris-flow initiation aligns with the regular distribution of repose time patterns, indicating a dependence of local process activity on sediment discharge and recharge. This stark difference in process behavior between our supply-limited site and transport-limited catchments has implications for assessing torrential hazard and risk mitigation in a context of global warming.

Debris flows are water-laden masses of rock, soil, air and fines with volumetric sediment concentrations typically exceeding 40%<sup>1–3</sup>. These sediment masses move rapidly through channel networks and across alluvial fans, where they claim lives and/or devastate property<sup>4–6</sup>. Debris flows are typically triggered by intense precipitation<sup>7–9</sup> and soil instability<sup>10–12</sup> occurring at the same locations periodically<sup>13</sup>. Studies on the historical development of debris flows, focusing almost exclusively on supply-unlimited catchments, point to an increase in both their frequency and magnitude<sup>14–17</sup> as a result of more frequent rainstorms, but also due to glacier retreat, rock-glacier acceleration<sup>18–20</sup>, or permafrost degradation<sup>21–24</sup> leading to enhanced accumulation of unconsolidated debris in the initiation zones of debris flows<sup>25</sup>. Yet, results are not unequivocal and some authors also argued that debris-flow activity does not show any clear trend at all<sup>21,26–29</sup> or even reduced activity<sup>30</sup> as a result of fewer storms in summer or changes in sediment supply. This conundrum<sup>31</sup> lies in part in the often complex – or indirect

– relation between debris-flow triggering, sediment availability, geomorphic connectivity, and climate<sup>32–34</sup>. Likewise, the scarcity of systematic data<sup>28,35,36</sup> hampers assessment of climate change impacts on debris flow occurrence, especially in remote mountain environments and over multi-centennial timescales<sup>28</sup>. In addition, the few datasets existing so far tend to suffer from non-uniform observation rates<sup>35</sup> as well as biases toward recent and larger debris flows causing damage to humans or infrastructure<sup>37–39</sup>. Major uncertainties therefore persist in (i) the assessment of multidecadal to centennial trends in debris-flow activity or (ii) the detection and attribution of climatic drivers which in turn influence changes in the frequency or magnitude of debris flows. These gaps in knowledge and observations currently also impede efforts to calibrate and evaluate process-based models that simulate the past and future evolution of debris-flow activity and impacts<sup>14,40</sup>. Here, we take advantage of an exceptional old-growth Swiss mountain pine (*Pinus mugo* ssp. *rotundata*) forest stand growing on the Multetta

<sup>1</sup>Climatic Change Impacts and Risks in the Anthropocene (C-CIA), Institute for Environmental Sciences, University of Geneva, 66 Boulevard Carl Vogt, CH-1205 Geneva, Switzerland. <sup>2</sup>dendrolab.ch, Department of Earth Sciences, University of Geneva, 13 rue des Maraichers, CH-1205 Geneva, Switzerland. <sup>3</sup>Université Grenoble Alpes, INRAE, CNRS, IRD, Grenoble INP, IGE, 2 rue de la Papeterie BP76, F-38402 Saint-Martin-d'Hères, France. <sup>4</sup>National Museum of Natural Sciences, MNCN-CSIC, C/ Serrano 115bis, E-28006 Madrid, Spain. <sup>5</sup>Department F.-A. Forel for Environmental and Aquatic Sciences, University of Geneva, 66 Boulevard Carl Vogt, CH-1205 Geneva, Switzerland. <sup>6</sup>Université Grenoble-Alpes, LECA UMR UGA-USMB-CNRS 5553, F-38058 Grenoble, Cedex 9, France.

✉ e-mail: [jiazhi.qie@etu.unige.ch](mailto:jiazhi.qie@etu.unige.ch); [markus.stoffel@unige.ch](mailto:markus.stoffel@unige.ch)

fan (Tschier, Grisons; Eastern Swiss Alps; 46.63°N, 10.31°E; Figs. 1 and 2). The stand is impacted by debris flows and thus suited for process reconstruction using dendrogeomorphic techniques<sup>41,42</sup>. This study does not only present the longest reconstruction of past debris-flow activity in the Eastern Swiss Alps, but also allows investigation of whether past and ongoing climate warming has had an impact on the frequency and magnitude of debris flows.

The Muletta fan (Figs. 1 and 2) is a massive depositional landform fed by four headwater catchments (Fig. 1B, Supplementary Fig. S1). Characterized by thin soils and low water storage capacity<sup>43</sup>, deposits consist of a main (surface: 1.03 km<sup>2</sup>) and a secondary fan (0.21 km<sup>2</sup>; Fig. 1B). Debris-flow material exclusively originates from the small (0.59 km<sup>2</sup>) but very steep (mean slope: 43.5°) *Vallun da Piz Daint* headwater catchment shown in Figs. 1C, 2, and Supplementary Fig. S2,

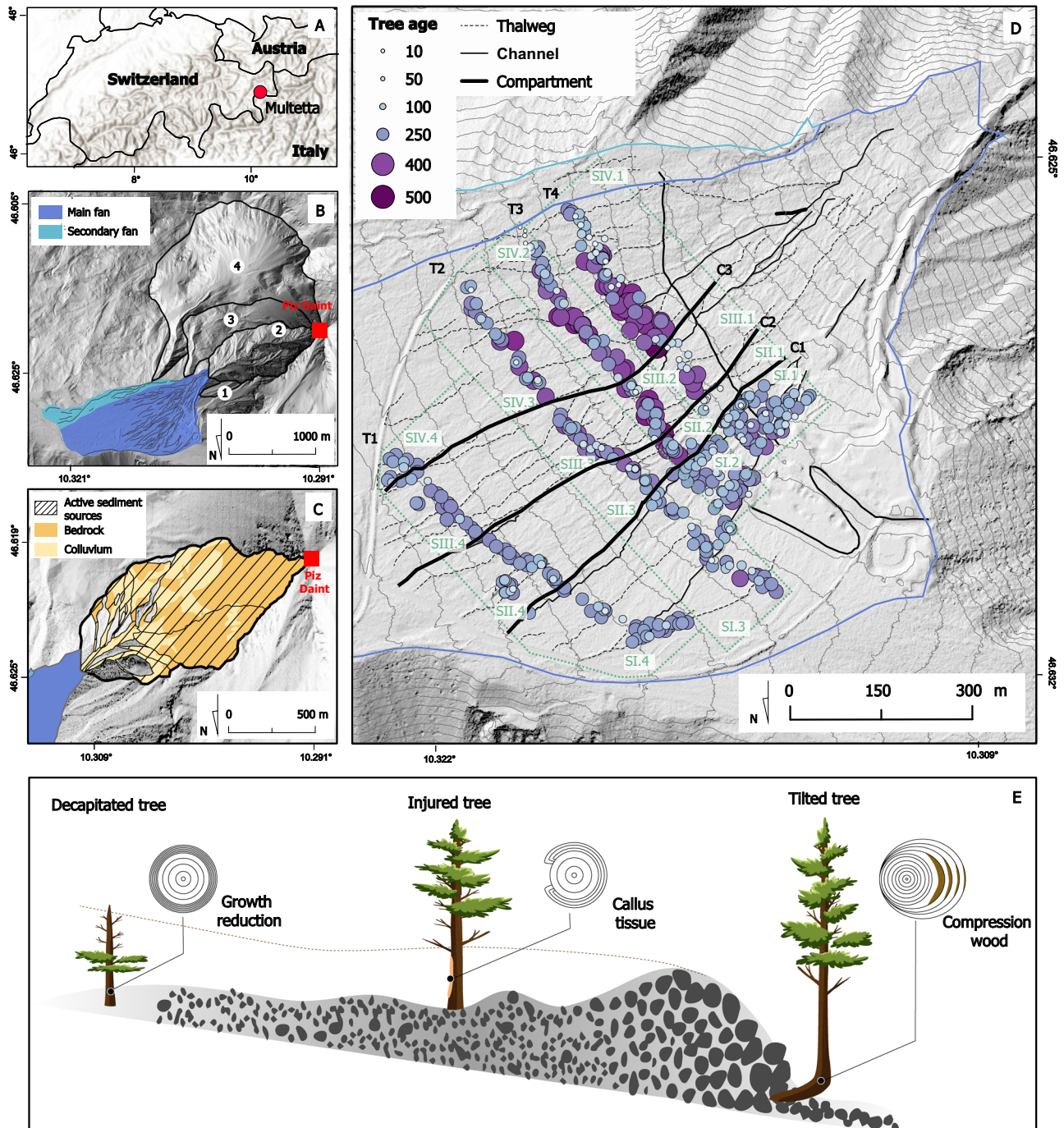


**Fig. 1 | Debris-flow activity reconstructed from multi-centennial, damaged Swiss mountain pines in a supply-limited catchment.** **A** The Muletta catchment is located in the Eastern Swiss Alps and **(B)** characterized by a main and a small secondary fan. The headwaters can be subdivided into four units, of which only unit 2 is directly connected to the fan. **C** This unit, known as *Vallun da Piz Daint* (reaching an elevation of up to 2968 m asl, red triangle) can be subdivided into 9 subunits, most of which consist of bedrock from which limited sediment is supplied to the

debris-flow system through freeze-thaw weathering. **D** On the main fan, a multi-centennial Swiss mountain pine (*Pinus mugo* ssp. *rotundata*) stand is regularly affected by debris flows. A total of 478 trees (colored dots) have been sampled here for dendrogeomorphic analyses along 4 transects. **E** Growth disturbances in Swiss mountain pine include growth reductions as well as the formation of callus tissue and compression wood after debris-flow impact; these changes in growth can be used to date events retrospectively with annual precision.



**Fig. 2 | Overview of the study site.** **A** Overview of the upper reaches of the Muletta fan with old-growth Swiss mountain pine (*Pinus mugo ssp. rotundata*) trees and debris-flow deposits (mostly levees in this case) and the poorly incised channels leading to frequent avulsions. The headwater catchment (Vallun da Piz Daint) can be seen in the background. **B** In the lower reaches of the Muletta fan, the relatively

fine debris-flow material injures and buries the pine trees, but does not necessarily kill them. As a result, the forest stand growing on the fan is unusually old and thus allows the construction of a long debris-flow timeseries. In this part of the fan, sequences of lobate deposits, levees and poorly marked channels dominate the landscape.

a feature underlain by Triassic sedimentary rocks of the Engadin Dolomites. Dominant lithologies consist of dolomites in the upper part, and sandstones in the lower part. Whereas the region was covered in ice during the Last Glacial Maximum, no glacial deposits exist anymore in the catchment, but can be found in its close vicinity. Permafrost is, at best, marginally present on the east face of Piz Daint<sup>44</sup> (2968 m asl, Fig. 1C). With a Melton index<sup>45</sup> of 1.24 and a proximal fan slope of 22%, the headwater catchment presents a very high debris-flow susceptibility<sup>46</sup>

Detailed analysis of orthoimages and LiDAR data indicates that Muletta is a debris-flow system with notable limitations in sediment supply. In fact, debris-flow activity is controlled by 9 active sediment sources representing 83% of Vallun da Piz Daint (Supplementary Fig. S2, Supplementary Table S1). These sources are dominated by rocky headwaters in which rockfall resulting from frost cracking is the main source of debris accumulation. In similar bedrock-dominated, low-order headwater catchments, loose debris has been shown to accumulate at a rate that is half that of colluvial erosion processes, with obvious consequences on debris-flow frequency<sup>47–49</sup>

## Results and discussion

### Multi-centennial debris flow reconstruction in the Eastern Swiss Alps

The eastern part of the main fan is covered with a continuous and dense *P. mugo* stand while on its western part, the forest is sparser and fragmented by recent debris-flow channels and deposits. Dendrogeomorphic analyses of the 478 *P. mugo* trees sampled along four

transects across the main fan (Fig. 1D) yield a mean tree age of  $261 \pm 85$  yrs and allowed detection of 1427 growth disturbances in the tree-ring series (Figs. 1E and 3A), corresponding to 56 years with debris-flow activity since 1626 CE (Fig. 3B). As the number of trees available for analysis decreases as one goes back in time and some parts of the fan may not have recording trees in the more distant past<sup>40,50</sup>, we realized a completeness analysis to assess the reliability of our data with two approaches<sup>50,51</sup> (see Methods). Results indicate that the period from which the tree-ring based reconstruction is reliable and free of biases commences in 1687 or 1750, depending on the approach used (Fig. 3B).

Considering successively 1687 ( $n=55$  events) and 1750 ( $n=44$  events) as starting dates of the reconstruction, we find a long-term average occurrence ratio of 0.16 and 0.2 debris flows year<sup>-1</sup>, respectively. Reconstructed process activity (Fig. 3B, Supplementary Fig. S3) points to an absence of events between 1750–1769, 1790–1799, 1850–1859, 1940–1950, and 2010–2019, whereas 0.4 debris flows year<sup>-1</sup> were recorded in the 1860s, 1890s and 1910s (Fig. 3B). Interestingly, all episodes with peaks in debris-flow activity are in line with those reported for the transport-limited, permafrost-dominated Ritigraben catchment (Valais, Western Swiss Alps)<sup>52</sup> and coincide with periods characterized by considerable above-average summer (JJA) and early fall (S) precipitation in the Swiss Alps<sup>53</sup>. Yet, and despite these decadal fluctuations in process activity at the Muletta fan, the Theil-Sen slope is zero for both the 1687–2020 and 1750–2020 datasets, clearly indicating an absence in changes in process activity. Likewise, we can neither reject a null hypothesis assuming the absence of a trend in the time series using the Bartels, Wald–Wolfowitz, and Mann–Kendall

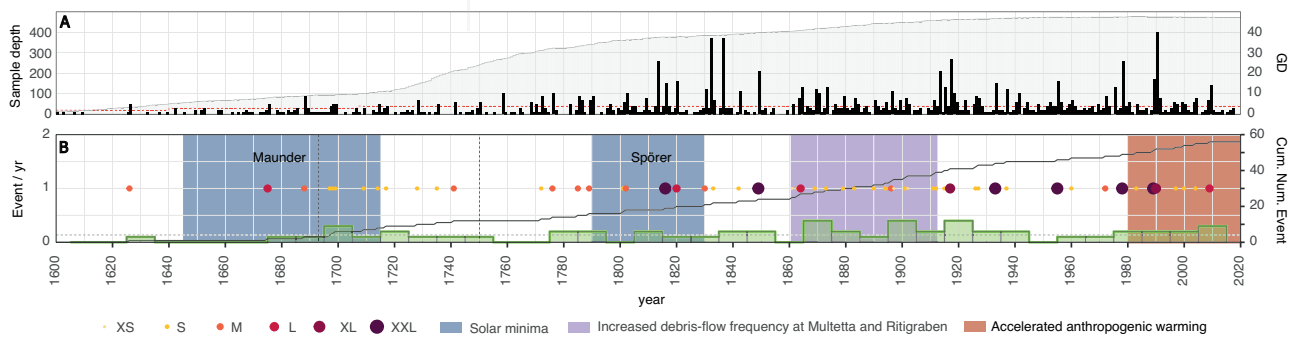


**Fig. 3 | At Multetta, debris-flow frequency and magnitude do not show any trend linked to climate variability and warming.** **A** Annual number of living trees (i.e. sample depth, gray area) and growth disturbances (GD, black bars) for the period 1600–2020. **B** Reconstructed debris flows (circles) and their relative magnitude shown as XS, S, M, L, XL and XXL (yellow-to-black color gradient). Completeness analyses suggest that the reconstruction is free of biases after 1687 or 1750 (vertical dotted lines), depending on the approach used. The black line depicts the cumulative number of debris flows; we do not find any breakpoint (see Methods) pointing to a change in debris-flow frequency over time. This absence of

anomalies is confirmed at decadal timescales (green bars) where the frequency of events ranges from 0 to 0.3 (mean = 0.16, horizontal dashed line). No clear control of temperature fluctuations on debris-flow activity can be evidenced during the coldest period of the Little Ice Age (blue rectangles) or as a result of the ongoing and accelerating warming climate (red rectangle). The purple surface shows the period spanning from the 1860s to the 1910s during which changes in debris-flow activity are similar between the Multetta (this study) and the Ritigraben (Western Swiss Alps) catchments.

trend tests ( $p$ -values > 0.05, Supplementary Table S2), nor detect a significant breakpoint in the cumulative number of events (Fig. 3B).

We also find that debris-flow frequency during the colder episodes of the Little Ice Age (LIA, 1570–1900<sup>54</sup>), known as the Maunder (1645–1715) and Dalton (1790–1830) minima, varied between zero debris flows year<sup>-1</sup> during the 1650s, 1660s and 1790s and 0.3 debris flows year<sup>-1</sup> in the 1690s. Unlike other studies according to which debris-flow activity is anticipated to increase as a result of climate change<sup>29,40</sup>, we do not detect any indications of enhanced process activity over the last decades that could potentially be linked to global warming (Fig. 3B).

### Spatial extent of reconstructed debris flows

Due to the massive redistribution of sediment on fans in space and time<sup>55,56</sup> and frequent avulsions, a precise reconstruction of the spatial extent of past debris-flow events is virtually impossible with tree-ring analysis<sup>2</sup>. In particular, the apparent spatial extent of events decreases once one goes back in time as fewer old trees will remain available for analysis<sup>57</sup> and as older deposits are routinely overridden by more recent activity<sup>58</sup>. Biases may also result from the annual resolution of tree-ring based reconstructions, often preventing detection of multiple debris flows occurring in a single year<sup>58,59</sup>. Here, we overcome these limitations by adopting an original approach by which the fan was schematically divided into sixteen units delimited by 4 transects and 4 radial subunits (see Methods for details) (Fig. 1D). Debris-flow sizes were defined as being XS, S, M, L, XL and XXL as soon as they affected 1–10, 10–20, 20–30, 30–40, 40–50 and >50% of the fan surface, respectively (see Methods). Since 1687, 4 (7%), 30 (55%), 9 (16%), 4 (7%), 2 (4%), and 6 (11%) debris flows were rated as XS, S, M, L, XL and XXL, respectively (Fig. 3B, Supplementary Fig. S4).

Over the period 1687–2009, as a result of the convex shape of the transverse profiles, recurrence intervals of debris flows were significantly lower at the margins (10–20 yr) than in the central part (40–70 yr) of the fan (Supplementary Fig. S4). Also, despite a homogeneous distribution of older trees on the fan, most debris flows were S or M prior to 1802 and restricted to the easternmost parts of the fan (Fig. 4B). The XXL events of 1816 and 1849 (Fig. 4A) strongly modified fan morphology and debris-flow patterns, resulting in a shift of activity to the western part of the fan from the mid-19<sup>th</sup> to the early 20<sup>th</sup> century (Fig. 4B, Supplementary Fig. S4). This shift recorded between the 1860s and 1910s and the slight increase in debris-flow activity were caused by a series of XS and S debris flows while larger debris flows

were lacking almost completely during this period (i.e. only 1L debris flow in 1864). We suggest that the slight increase in debris-flow frequency during this time was possible because the many debris flows remained (very) small in size and could not therefore empty the sediment reservoirs at Vallun da Piz Daint fully. By contrast, in the transport-limited, permafrost-dominated Ritigraben catchment<sup>52</sup>, multiple L and XL debris flows were reconstructed for the same period. Here, changes in the frequency and magnitude of debris flows are considered the response of the system to more abundant summer precipitation and initial warming after the end of the Little Ice Age.

During the 20<sup>th</sup> and early 21<sup>st</sup> centuries, any evidence for a change in process activity or an increase in the occurrence of XL and XXL debris flows are clearly lacking at Multetta (Fig. 3B), and we note a complete absence of L, XL or XXL debris flows since 1990. By contrast, ample evidence exists for the repeat activation of new paths in the northern and southern parts of the fan after the debris flows of 1917 and 1933 (Fig. 4A, B, Supplementary Fig. S3). The spatial patterns of debris-flow activity at the site also confirm that avulsions are typically encouraged by sequences of small-to-medium-sized debris flows followed by a large event<sup>2,60,61</sup>.

### Sediment availability and time-repose patterns

Debris-flow frequency of a catchment is, besides climatic thresholds, also controlled by geological, lithological and geomorphic characteristics<sup>56,62</sup>. Initiation mechanisms of debris flows include the transition of landslides into debris flows<sup>63–65</sup>, the entrainment and bulking of sediment in loose deposits at the toe of a cliff<sup>56,67</sup> or the mobilization and entrainment of debris by water in channels<sup>68,69</sup>. Sediment availability must thus be considered another key controlling process variable for inter-event (repose) intervals of debris flows<sup>62</sup>.

Whereas in transport-limited basins, an almost unlimited availability of sediment usually results in irregular, random repose time patterns following an exponential distribution<sup>62</sup>, regular or clustered repose time patterns are typically observed in supply-limited basins where a substantial time must elapse before the next debris flow will occur following log-logistic and Weibull distributions. In the case of the Multetta fan, the Weibull distribution provides the best-fitting results ( $p$ -value > 0.05 and lowest AIC) for both an initial date of the reconstructed timeseries in 1687 and 1750 (Fig. 5A, B). Likewise, the conditional probability for the occurrence of a new debris flow increases slightly with time elapsed since the last event. The regular event occurrence reflects the mutual dependency between

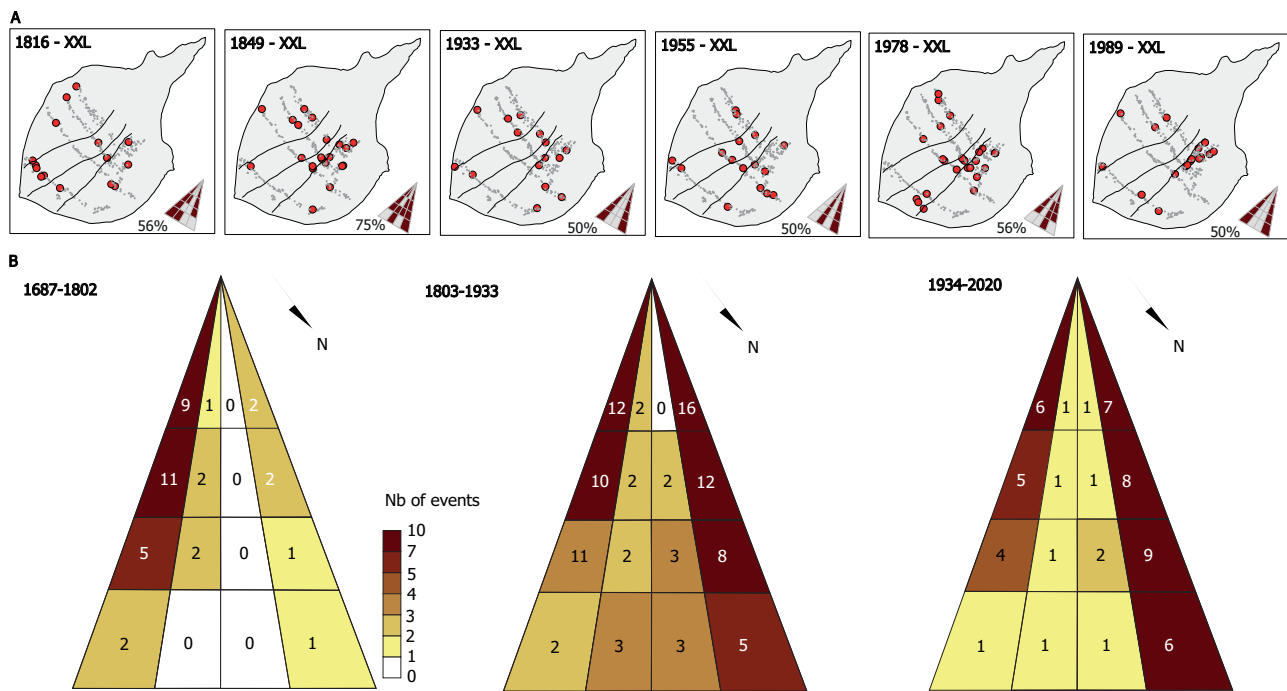


**Fig. 4 | Major debris flows resulted in substantial reconfigurations of fan morphology.** **A** XXL debris flows reconstructed in 1816, 1849, 1933, 1955, 1978 and 1989 affected 50–75% of the fan analyzed. Gray and red dots indicate living and impacted trees, respectively. Brown areas in the inset figure point to the surface

affected by a debris flow in any given year. **B** XXL events also resulted in major avulsions, thereby changing in pathways of debris flows from the eastern to the western margins of the fan.

consecutive debris flows and highlights that the cut-and-fill pattern, i.e. the time for the system to replenish after a debris-flow event<sup>70–72</sup>, is a key control of debris-flow activity at the Multetta fan.

Theoretical understanding exists that possible changes in the number, duration, or intensity of freeze-thaw cycles due to warming could increase sediment supply in high-mountain catchments<sup>73–75</sup>. The headwaters of the Multetta debris-flow system are indeed found at elevations for which changes in freeze-thaw cycles are thought to be relevant<sup>75</sup>. Yet, and despite local warming already exceeding 2 °C since the late 19<sup>th</sup> century, we cannot detect any changes of a possibly altered sediment availability on debris-flow activity so far.

Debris flow is one of the dominant geomorphic processes in mountainous regions, yet, its documentation or the detection of changes in process activity remains challenging due to the paucity of systematic, long-term records of past events<sup>28,35</sup>. Here we overcome this limitation by reconstructing the systematic, multi-centennial (1626–2020) timeseries of debris flows for a supply-limited catchment where process activity is not affected by the provision of unlimited sediment from thawing permafrost or retreating glaciers. Relying on data from the Multetta, we demonstrate that debris flows in this supply-limited system recur less frequently than in comparable, transport-limited catchments. In addition, the regular recurrence of debris flows and the resulting repose time patterns also evidence that process activity is controlled by sediment supply over multi-decadal to centennial timescales and thus much less affected by climate change than transport-limited systems<sup>62</sup>. Findings from this study have implications for future torrent management as the implementation of climate-proof measures (e.g., enlargement of hazard zones, re-dimensioning of defense structures<sup>76</sup>) should be defined based on sediment availability and the functioning of the debris-flow system.

## Methods

### Limited sediment supply confirmed by geomorphic mapping

To determine the functioning of the Multetta debris-flow system and the production/availability of sediment, we realized a detailed

mapping of active sediment sources for its headwaters, i.e. the Vallun da Piz Daint. Active sediment sources were defined here as unvegetated and steep hillslope surfaces where active geomorphic processes can be detected, and where connectivity to the main channel arriving at the fan apex can be confirmed. This was done by aerial photo interpretation of orthoimages (2022, resolution 10 cm) and the hillshade view of a Light Detection and Range (LiDAR) Digital Elevation Model (DEM; 2023, resolution 1 m) available from Swisstopo. The high quality of these remote sensing data allowed manual extraction of bedrock and colluvium surfaces for the entire catchment, and calculation of the relative surface of these geomorphic domains for each active sediment source. Colluvial deposits in the catchment included scree slopes, debris-flow and colluvial fans, and a large rockfall deposit.

### Dendrogeomorphic sampling at Multetta fan

Debris flows are the predominant process at Multetta and have formed characteristic geomorphic features, such as lobes, levees bank erosion and terraces. In the forest virtually every tree shows clear evidence of past debris flow impact on the stem surface, predominantly in the form of injuries or broken crowns. To gather a representative dataset of past debris flow activity, we sampled trees along four transects (T1–T4) located at 1800–1900, 1784–1900, 1780–1900, 1790–1900 m asl, respectively (Fig. 1C). On each transect, trees were carefully inspected and sampled based on visible growth disturbances (GDs) on the stem (i.e. scars, decapitation, tilted stems). Two increment cores were taken from living trees, using a 5.5 mm Pressler increment borer, following the assumed direction of past debris flow events. For visible scars, additional cores or wedges were taken in the overgrowing callus tissue. For tilted trees, cores were taken at the point of maximum stem bending<sup>77</sup>. Cross sections were taken from dead trees and stumps. Trees with growth disturbances (GDs) obviously unrelated to debris flows (e.g., injuries caused by a falling neighboring tree) due to their incoherent position on the stem were systematically excluded. The position of each sampled tree positions was recorded with an accuracy

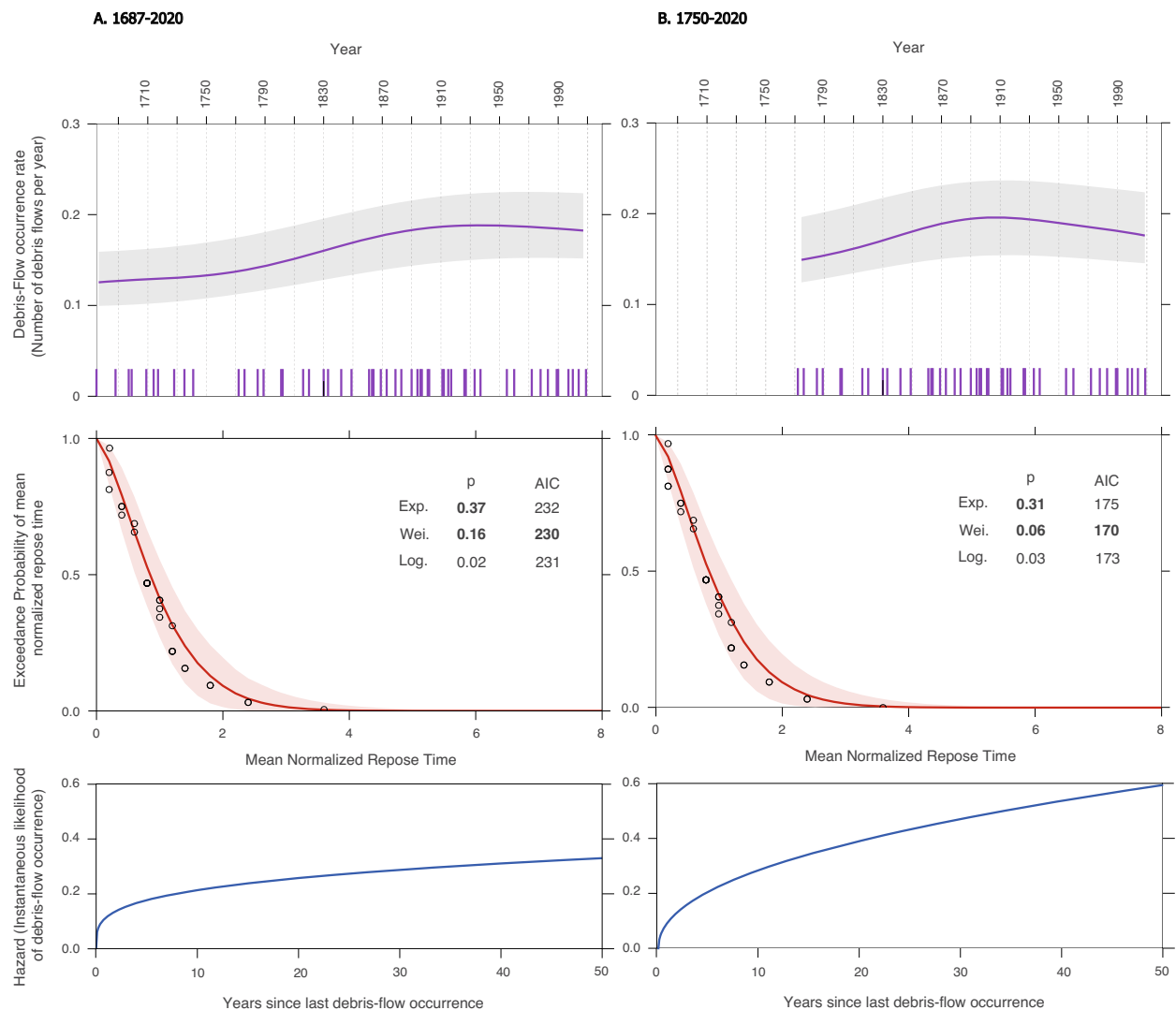


**Fig. 5 | Best-fitting distributions of repose-time patterns at Mulletta fan over the period. A** 1687–2020 and **B** 1750–2020 are given by the Weibull distribution ( $p > 0.05$ , lowest Akaike information criterion (AIC)), pointing to regular and dependent debris-flow repose times as typical for supply-limited catchments. The upper/central panels show estimated annual debris-flow occurrence rates and corresponding estimated repose time distributions. All repose times were normalized by dividing them by their mean value. The general suitability of the

distributions was tested with the p-value associated to a Monte Carlo version of the Kolmogorov–Smirnov test. The distribution with the lowest AIC value (i.e. Weibull in our case) is shown with a pointwise 95% confidence interval based on 1000 bootstrap samples<sup>62</sup>. The bottom panel shows the likelihood for a debris flow to occur at a certain time lag after the last event based on the hazard function of the Weibull distribution<sup>62</sup>.

of 1 m using a Trimble GPS device. In total of 478 *P. mugo* trees were sampled during a field campaign in 2020.

### Laboratory analyses

In the laboratory, tree samples were processed according to the standard procedures<sup>78</sup>. Ring widths were measured on the scanned images and series were cross-dated using the CDendro-CooRecorder 9.8.1 software suite<sup>79</sup>. The quality of the cross-dating was evaluated using COFECHA<sup>80</sup>. Within each ring width series, we identified GDs commonly interpreted as responses to geomorphic processes including abrupt growth suppression<sup>81</sup> (GS), the onset of compression wood<sup>82</sup> (CW) and injuries<sup>83</sup> (I). Following the criteria proposed by ref. 84, the intensity of GS and CW was categorized as weak, medium or strong according. Injuries, GS and CW of medium and strong intensity were considered as unambiguous witnesses of debris flows and used for event detection. The first 30 rings of each tree-ring series, corresponding to juvenile growth, were not included in the analysis, because young flexible trees, which are more susceptible to bending,

could potentially bias the reconstruction<sup>85</sup>. Only one core per tree was analyzed if the other one did not show obvious GDs, finally 478 *P. mugo* trees with 683 increment cores and 39 cross sections/wedges were proceeded to build the debris flow chronology.

### Zonation of the study area

To account for the wide area and the geomorphic complexity of the fan, prior to event detection, we divided the study area in different sectors (Fig. 1D). For this purpose, we identified the main fan-surface topographic features, including channels, main lobes, and levees, on a Digital Elevation Model (DEM) hillshade with 2-m spatial resolution created from a lidar point cloud. We determined the position of the channels using the flow accumulation tool available from the arc-hydro module of ESRI ArcGIS 10.7. Based on the 2-m DEM, the tool calculates accumulated flow as the accumulated weight of all cells flowing into each downslope cell in the output raster. Cells were selected by applying a 1200 mm accumulation threshold and were divided into channels and thalwegs. Based on this analysis, we further identified

three compartments (C1–C3) manually following the flow directions and the continuities of the river networks on the Muletta fan (Fig. 1D). These thalwegs distributed almost parallelly, connect the proximal and the distal area of the fan in the southeastern part and initiate at ~1900 m asl on its northeastern part. They delimit four sectors (SI–SIV) in which debris flows were reconstructed.

### Detection of past debris flow events

In each sector SI–SIV, the detection of past debris flow events was based on (1) the number, (2) the intensity of GDs the (3) percentage ( $It$ )<sup>86</sup> and (4) the spatial patterns of damaged within a given year. The reconstructions starts when the minimum number of trees exceeds 15. Following the recommendations of Ref. 87, we used flexible  $It$  and GD thresholds adjusted to the sample size ( $ss$ ):  $GDs \geq 2$ ,  $It \geq 6$  for  $ss < 50$ ,  $GDs \geq 3$  and  $It \geq 4$  for  $50 < ss \leq 99$ , as  $GDs \geq 4$  and  $It \geq 2$  for  $ss \geq 100$ . Following ref. 88, we quantified the robustness of reconstructed events (low, medium, and high confidence levels) based on the intensity of GDs within a given year. In a final step, we carefully examined the spatial distribution of damaged trees. Years (1) showing incoherent patterns of damaged trees (e.g. GDs evenly distributed on the cone, probably due to climatic extremes or insect pests), (2) recorded in historical chronicles as snow avalanche years, or (3) characterized by high mortality of *P. mugo* trees, which is indicated by low tree-ring index (<1.5 average value), in the event cataster of the Canton of Grisons and the Swiss National Park<sup>89</sup> were excluded from analysis. To detect changes in the reconstruction potentially related to time-varying sample size<sup>87,90</sup>, we performed a completeness analysis using Negative Binomial and non-parametric change-point analyses<sup>50,91</sup> available from the `np` package in R.

### Spatial extent of reconstructed events

Due to the intense redistribution of sediments through space and time on debris-flow fans and the frequent avulsions, precise reconstructions of the spatial extent of past debris events are impossible using tree-ring analysis<sup>2</sup>. In fact, the spatial extent of events, decreases with age because of fewer old trees<sup>57</sup>. In addition, part of older deposits may be overridden or eroded by more recent activity. A smaller number of affected trees may thus not imply that those older events were smaller than more recent flows<sup>37</sup>. Finally, as tree-ring resolution is typically annual, it must be assumed that all trees affected within a given year were affected by the same event. This may be restrictive assumption if the typical return period of debris flows is on the order of decades to centuries<sup>58</sup>. To overcome these limitations, we adopted an original approach and schematically divided the cone into sixteen regions delimited by the four sectors (SI–SIV) used for event detection and the four transects used for sampling (T1–T4, Fig. 1D). For a given year, a given region (SI.1–S.IV.4) was considered as affected if (1) an event was reconstructed in the sector and (2) a tree was damaged on the transect T1–T4. Within a given area, the recurrence interval of debris flow events was calculated as the ratio of the length of the reconstruction to the number of reconstructed events. Finally, if 1–10, 10–20, 20–30, 30–40, 40–50 and >50% of the areas were affected, the magnitude of the event was classified as XS, S, M, L, XL, XXL (Fig. 4A).

### Trends in debris flow activity

There is currently much debate about the impacts of global warming on the frequency of debris flows<sup>37,91,92</sup>. An increase in frequency is expected due to the increasing frequency of extreme precipitation events<sup>93</sup>, warming and thawing of permafrost<sup>29</sup>, but remains controversial in historical records<sup>94,95</sup> or tree-ring reconstructions<sup>27,51</sup>. Here, we took advantage of the age of the trees on the debris fan and of the multi-century length of our reconstruction, to perform several (nonparametric) trend tests for assessing the presence of trends in the decadal frequency of debris flow events. Following refs. 50,91, we used the nonparametric Mann–Kendall, Wald–Wolowitz trends test and the

Theil–Sen slope for assessing the presence of trends in the data set over the 1687–2020 and 1750–2020 periods.

### Repose-time patterns of debris flow events at Muletta

A significant contributor to debris-flow occurrence is a supply of readily erodible material, often created by rockfalls and landslides<sup>71</sup>. In general, debris-flow catchments can be classified as either supply-unlimited (transport-limited) or supply-limited (weathering-limited). Depending on the available sediment load, debris-flow repose times, i.e. the time elapsed between two consecutive events, follow either more or less regular (supply-limited), rather irregular or purely irregular (supply-unlimited) occurrence patterns<sup>62,96,97</sup>. Following Ref. 62, we hypothesize that when events occur continuously and independently at a constant average rate, repose times should be exponentially distributed. By contrast, debris flow event frequencies showing regular or rather irregular (clustered) repose time patterns, indicating potential dependencies between events, could be efficiently modeled with respect to a Weibull or a log-logistic distribution, respectively. The three distributions were successively used to model the frequency of the repose times at the Muletta fan. Distributions yielding a *p*-value larger than 0.05 were considered suitable and the best-suited distribution was chosen on the basis on the lowest Akaike information criterion (AIC).

### Data availability

The base maps in Fig. 1, Figure S1 and Figure S2 were produced using free geodata from the Federal Office of Topography `swisstopo` <https://www.swisstopo.admin.ch/>. All tree-ring data, growth disturbance data and final debris-flow chronology data generated in this study have been deposited in the database named “Climate change has no apparent effect on debris flows in a supply-limited torrent” under accession code <https://doi.org/10.5281/zenodo.13745071>.

### Code availability

The R code used for completeness analysis in this study is originally from the previously published paper<sup>51</sup> and is available on GitLab at <https://gitlab.com/Rexthor/debris-flow-trends-zermatt>. The R code used for repose time pattern analysis in this study is originally from the previously published paper<sup>62</sup> and is available on GitLab at <https://gitlab.com/Rexthor/repose-time-patterns>.

### References

- Calhoun, N. C. & Clague, J. J. Distinguishing between debris flows and hyperconcentrated flows: an example from the eastern Swiss Alps: Bonaduz mass flow. *Earth Surf. Process. Landf.* **43**, 1280–1294 (2018).
- De Haas, T. et al. Avulsions and the spatio-temporal evolution of debris-flow fans. *Earth Sci. Rev.* **177**, 53–75 (2018).
- Iverson, R. M. The physics of debris flows. *Rev. Geophys.* **35**, 245–296 (1997).
- Iverson, R. M. Debris flows: behaviour and hazard assessment. *Geol. Today* **30**, 15–20 (2014).
- Cruden, D. Debris-flow hazards and related phenomena. *Can. Geotech. J.* **42**, 1723 (2005).
- Dowling, C. A. & Santi, P. M. Debris flows and their toll on human life: a global analysis of debris-flow fatalities from 1950 to 2011. *Nat. Hazards* **71**, 203–227 (2014).
- Guzzetti, F., Peruccacci, S., Rossi, M. & Stark, C. P. The rainfall intensity–duration control of shallow landslides and debris flows: an update. *Landslides* **5**, 3–17 (2008).
- Palladino, M. R. et al. Rainfall thresholds for the activation of shallow landslides in the Italian Alps: the role of environmental conditioning factors. *Geomorphology* **303**, 53–67 (2018).
- Marchi, L. et al. Debris flows recorded in the Moscardo catchment (Italian Alps) between 1990 and 2019. *Nat. Hazards Earth Syst. Sci.* **21**, 87–97 (2021).

10. Blijenberg, H. M. Application of physical modelling of debris flow triggering to field conditions: Limitations posed by boundary conditions. *Eng. Geol.* **91**, 25–33 (2007).
11. Du, J., Fan, Z., Xu, W. & Dong, L. Research Progress of Initial Mechanism on Debris Flow and Related Discrimination Methods: A Review. *Front. Earth Sci.* **9**, 629567 (2021).
12. Imaizumi, F., Sidle, R. C., Tsuchiya, S. & Ohsaka, O. Hydrogeomorphic processes in a steep debris flow initiation zone: HYDROGEOMORPHOLOGY OF DEBRIS FLOW SITES. *Geophys. Res. Lett.* **33**, (2006).
13. Turnbull, B., Bowman, E. T. & McElwaine, J. N. Debris flows: Experiments and modelling. *Comptes Rendus Phys.* **16**, 86–96 (2015).
14. Hock, R. et al. High Mountain Areas. in *IPCC Special Report on the Ocean and Cryosphere in a Changing Climate* (IPCC, 2019).
15. Dietrich, A. & Krautblatter, M. Evidence for enhanced debris-flow activity in the Northern Calcareous Alps since the 1980s (Plansee, Austria). *Geomorphology* **287**, 144–158 (2017).
16. Winter, M. G. Chapter 5 Debris flows. *EGSP* **29**, 163–185 (2020).
17. Kiefer, C. et al. A 4000-year debris flow record based on amphibious investigations of fan delta activity in Plansee (Austria, Eastern Alps). *Earth Surf. Dynam.* **9**, 1481–1503 (2021).
18. Stoffel, M. & Graf, C. Debris-flow activity from high-elevation, periglacial environments. In *The High-Mountain Cryosphere* (eds. Huggel, C., Carey, M., Clague, J. J. & Käab, A.) 295–314 (Cambridge University Press, 2015). <https://doi.org/10.1017/CBO9781107588653.016>.
19. Eriksen, H. Ø. et al. Recent Acceleration of a Rock Glacier Complex, Ådjet, Norway, Documented by 62 Years of Remote Sensing Observations. *Geophys. Res. Lett.* **45**, 8314–8323 (2018).
20. Wirz, V., Geertsema, M., Gruber, S. & Purves, R. S. Temporal variability of diverse mountain permafrost slope movements derived from multi-year daily GPS data, Mattertal, Switzerland. *Landslides* **13**, 67–83 (2016).
21. Stoffel, M., Mendlik, T., Schneuwly-Bollschiweiler, M. & Gobiet, A. Possible impacts of climate change on debris-flow activity in the Swiss Alps. *Clim. Change* **122**, 141–155 (2014).
22. De Haas, T., Kleinhans, M. G., Carbonneau, P. E., Rubensdotter, L. & Hauber, E. Surface morphology of fans in the high-Arctic periglacial environment of Svalbard: Controls and processes. *Earth Sci. Rev.* **146**, 163–182 (2015).
23. Jakob, M. & Friele, P. Frequency and magnitude of debris flows on Cheekye River, British Columbia. *Geomorphology* **114**, 382–395 (2010).
24. Li, M. et al. Impacts of future climate change (2030–2059) on debris flow hazard: A case study in the Upper Minjiang River basin, China. *J. Mt. Sci.* **15**, 1836–1850 (2018).
25. Savi, S., Comiti, F. & Strecker, M. R. Pronounced increase in slope instability linked to global warming: A case study from the eastern European Alps. *Earth Surf. Process. Landf.* **46**, 1328–1347 (2021).
26. Stoffel, M. et al. 400 Years of Debris-Flow Activity and Triggering Weather Conditions: Ritigraben, Valais, Switzerland. *Arct. Antarct. Alp. Res.* **37**, 387–395 (2005).
27. Bollschiweiler, M. & Stoffel, M. Changes and trends in debris-flow frequency since AD 1850: Results from the Swiss Alps. *Holocene* **20**, 907–916 (2010).
28. Rom, J. et al. Spatio-temporal analysis of slope-type debris flow activity in Horlachtal, Austria, based on orthophotos and lidar data since 1947. *Nat. Hazards Earth Syst. Sci.* **23**, 601–622 (2023).
29. Turkington, T., Remaître, A., Ettema, J., Hussin, H. & Van Westen, C. Assessing debris flow activity in a changing climate. *Clim. Change* **137**, 293–305 (2016).
30. Hirschberg, J. et al. Climate Change Impacts on Sediment Yield and Debris-Flow Activity in an Alpine Catchment. *J. Geophys. Res. Earth Surf.* **126**, e2020JF005739 (2021).
31. Huggel, C., Clague, J. J. & Korup, O. Is climate change responsible for changing landslide activity in high mountains? *Earth Surf. Process. Landf.* **37**, 77–91 (2012).
32. Crozier, M. J. Deciphering the effect of climate change on landslide activity: A review. *Geomorphology* **124**, 260–267 (2010).
33. Marchi, L., Brunetti, M. T., Cavalli, M. & Crema, S. Debris-flow volumes in northeastern Italy: Relationship with drainage area and size probability. *Earth Surf. Process. Landf.* **44**, 933–943 (2019).
34. Micheletti, N., Lambiel, C. & Lane, S. N. Investigating decadal-scale geomorphic dynamics in an alpine mountain setting. *J. Geophys. Res. Earth Surf.* **120**, 2155–2175 (2015).
35. Marchi, L. & Tecca, P. R. Some Observations on the Use of Data from Historical Documents in Debris-Flow Studies. *Nat. Hazards* **38**, 301–320 (2006).
36. Harrison, A. & Dashwood, C. Climate change and geohazards. *Nat. Clim. Chang.* **14**, 553–554 (2024).
37. Gariano, S. L. & Guzzetti, F. Landslides in a changing climate. *Earth Sci. Rev.* **162**, 227–252 (2016).
38. Tropeano, D. & Turconi, L. Using Historical Documents for Landslide, Debris Flow and Stream Flood Prevention. Applications in Northern Italy. *Nat. Hazards* **31**, 663–679 (2004).
39. D’Agostino, V. & Marchi, L. Debris flow magnitude in the Eastern Italian Alps: data collection and analysis. *Phys. Chem. Earth Part C Sol. Terrestrial Planet. Sci.* **26**, 657–663 (2001).
40. Kaitna, R. et al. Changes of hydro-meteorological trigger conditions for debris flows in a future alpine climate. *Sci. Total Environ.* **872**, 162227 (2023).
41. Stoffel, M. & Corona, C. Dendroecological Dating of Geomorphic Disturbance in Trees. *Tree Ring Res.* **70**, 3–20 (2014).
42. Šilhán, K. Historical activity of debris flows in the medium-high mountains: Regional reconstruction using dendrogeomorphic approach. *Sci. Total Environ.* **856**, 159248 (2023).
43. Baumann, F. & Kaiser, K. F. The Multetta Debris Fan, Eastern Swiss Alps: A 500-year Debris Flow Chronology. *Arct. Antarct. Alp. Res.* **31**, 128–134 (1999).
44. Gruber, S. & Hoelzle, M. Statistical modelling of mountain permafrost distribution: local calibration and incorporation of remotely sensed data. *Permafr. Periglac. Process.* **12**, 69–77 (2001).
45. Melton, M. A. The Geomorphic and Paleoclimatic Significance of Alluvial Deposits in Southern Arizona. *J. Geol.* **73**, 1–38 (1965).
46. Bertrand, M., Liébault, F. & Piégay, H. Debris-flow susceptibility of upland catchments. *Nat. Hazards* **67**, 497–511 (2013).
47. Brardinoni, F., Church, M., Simoni, A. & Macconi, P. Lithologic and glacially conditioned controls on regional debris-flow sediment dynamics. *Geology* **40**, 455–458 (2012).
48. Theule, J. I., Liébault, F., Loye, A., Laigle, D. & Jaboyedoff, M. Sediment budget monitoring of debris-flow and bedload transport in the Manival Torrent, SE France. *Nat. Hazards Earth Syst. Sci.* **12**, 731–749 (2012).
49. Loye, A., Jaboyedoff, M., Theule, J. I. & Liébault, F. Headwater sediment dynamics in a debris flow catchment constrained by high-resolution topographic surveys. *Earth Surf. Dynam.* **4**, 489–513 (2016).
50. Heiser, M., Hübl, J. & Scheidl, C. Completeness analyses of the Austrian torrential event catalog. *Landslides* **16**, 2115–2126 (2019).
51. Heiser, M., Schlögl, M., Scheidl, C. & Fuchs, S. Comment on “Hydrometeorological Triggers of Periglacial Debris Flows in the Zermatt Valley (Switzerland) Since 1864” by Michelle Schneuwly-Bollschiweiler and Markus Stoffel. *JGR Earth Surface* **127**, e2021JF006562 (2022).
52. Stoffel, M. & Beniston, M. On the incidence of debris flows from the early Little Ice Age to a future greenhouse climate: A case study from the Swiss Alps. *Geophys. Res. Lett.* **33**, L16404 (2006).
53. Pfister, C., Luterbacher, J. & Wanner, H. *Wetternachhersage: 500 Jahre Klimavariationen Und Naturkatastrophen (1496-1995)* (P. Haupt, Bern, 1999).



54. Grove, J. M. *Little Ice Ages: Ancient and Modern* (Routledge, 2019). <https://doi.org/10.4324/9780203505205>.
55. Hungr, O., Evans, S. G., Bovis, M. J. & Hutchinson, J. N. A review of the classification of landslides of the flow type. *Environ. Eng. Geosci.* **7**, 221–238 (2001).
56. Zhao, T., Zhou, G. D., Sun, Q., Crosta, G. B. & Song, D. Slope erosion induced by surges of debris flow: insights from field experiments. *Landslides* **19**, 2367–2377 (2022).
57. Stoffel, M., Conus, D., Grichting, M. A., Lièvre, I. & Maître, G. Unraveling the patterns of late Holocene debris-flow activity on a cone in the Swiss Alps: Chronology, environment and implications for the future. *Glob. Planet. Change* **60**, 222–234 (2008).
58. Schneuwly-Bollschiweiler, M. & Stoffel, M. Hydrometeorological triggers of periglacial debris flows in the Zermatt valley (Switzerland) since 1864. *J. Geophys. Res. Earth Surf.* **117**, (2012).
59. Van Steijn, H. Debris-flow magnitude—frequency relationships for mountainous regions of Central and Northwest Europe. *Geomorphology* **15**, 259–273 (1996).
60. Densmore, A. L., De Haas, T., McArdell, B. W. & Schuerch, P. Making sense of avulsions on debris-flow fans, <https://doi.org/10.25676/1124/173161> (2019).
61. Haas, T., Densmore, A. L., Hond, T. & Cox, N. J. Fan-Surface Evidence for Debris-Flow Avulsion Controls and Probabilities, Saline Valley, California. *J. Geophys. Res. Earth Surf.* **124**, 1118–1138 (2019).
62. Heiser, M. et al. Repose time patterns of debris-flow events in alpine catchments. *Earth Surf. Process. Land.* **48**, 1034–1051 (2023).
63. Wieczorek, G. F. Effect of rainfall intensity and duration on debris flows in central Santa Cruz Mountains, California. In *Reviews in Engineering Geology* vol. 7 93–104 (Geological Society of America, 1987).
64. Imaizumi, F. & Sidle, R. C. Linkage of sediment supply and transport processes in Miyagawa Dam catchment, Japan. *J. Geophys. Res.* **112**, F03012 (2007).
65. Berger, C., McArdell, B. W. & Schlunegger, F. Sediment transfer patterns at the Illgraben catchment, Switzerland: Implications for the time scales of debris flow activities. *Geomorphology* **125**, 421–432 (2011).
66. Larsen, I. J., Pederson, J. L. & Schmidt, J. C. Geologic versus wildfire controls on hillslope processes and debris flow initiation in the Green River canyons of Dinosaur National Monument. *Geomorphology* **81**, 114–127 (2006).
67. Coe, J. A., Kinner, D. A. & Godt, J. W. Initiation conditions for debris flows generated by runoff at Chalk Cliffs, central Colorado. *Geomorphology* **96**, 270–297 (2008).
68. Berti, M., Genevois, R., Simoni, A. & Tecca, P. R. Field observations of a debris flow event in the Dolomites. *Geomorphology* **29**, 265–274 (1999).
69. Cannon, S. H. & Reneau, S. L. Conditions for generation of fire-related debris flows, Capulin Canyon, New Mexico. *Earth Surf. Process. Landf.* **25**, 1103–1121 (2000).
70. Jakob, M. & Bovis, M. *Morphometric and geotechnical controls of debris flow activity, southern Coast Mountains, British Columbia, Canada*, Supplement-Band 13–26 (Zeitschrift für Geomorphologie, N.F., 1996).
71. Jakob, M., Holm, K. & McDougall, S. Debris-Flow Risk Assessment. in *Oxford Research Encyclopedia of Natural Hazard Science* (Oxford University Press, 2016). <https://doi.org/10.1093/acrefore/9780199389407.013.37>.
72. Bonneau, D. A., Hutchinson, D. J., McDougall, S., DiFrancesco, P.-M. & Evans, T. Debris-Flow Channel Headwater Dynamics: Examining Channel Recharge Cycles With Terrestrial Laser Scanning. *Front. Earth Sci.* **10**, 883259 (2022).
73. Morel, M., Piton, G., Kuss, D., Evin, G. & Le Bouteiller, C. Statistical Modelling of Sediment Supply in Torrent Catchments of the Northern French Alps. *Nat. Hazards Earth Syst. Sci.* **23**, 1769–1787 (2023).
74. Deprez, M., De Kock, T., De Schutter, G. & Cnudde, V. A review on freeze-thaw action and weathering of rocks. *Earth Sci. Rev.* **203**, 103143 (2020).
75. Mayer, T., Deprez, M., Schröder, L., Cnudde, V. & Draebing, D. Quantifying frost-weathering-induced damage in alpine rocks. *Cryosphere* **18**, 2847–2864 (2024).
76. Staffler, H., Pollinger, R., Zischg, A. & Mani, P. Spatial variability and potential impacts of climate change on flood and debris flow hazard zone mapping and implications for risk management. *Nat. Hazards Earth Syst. Sci.* **8**, 539–558 (2008).
77. Bollschiweiler, M., Stoffel, M. & Schneuwly, D. Dynamics in debris-flow activity on a forested cone — A case study using different dendroecological approaches. *CATENA* **72**, 67–78 (2008).
78. Bräker, O. U. Measuring and data processing in tree-ring research — a methodological introduction. *Dendrochronologia* **20**, 203–216 (2002).
79. Maxwell, R. S. & Larsson, L.-A. Measuring tree-ring widths using the CooRecorder software application. *Dendrochronologia* **67**, 125841 (2021).
80. Holmes, R. L. *Dendrochronology program manual*. (UWICER Press, 1994).
81. Bollschiweiler, M., Stoffel, M., Ehmisch, M. & Monbaron, M. Reconstructing spatio-temporal patterns of debris-flow activity using dendrogeomorphological methods. *Geomorphology* **87**, 337–351 (2007).
82. Šilhán, K. & Stoffel, M. Impacts of age-dependent tree sensitivity and dating approaches on dendrogeomorphic time series of landslides. *Geomorphology* **236**, 34–43 (2015).
83. Schneuwly, D. M. & Stoffel, M. Tree-ring based reconstruction of the seasonal timing, major events and origin of rockfall on a case-study slope in the Swiss Alps. *Nat. Hazards Earth Syst. Sci.* **8**, 203–211 (2008).
84. Kogelnig-Mayer, B., Stoffel, M., Schneuwly-Bollschiweiler, M., Hübl, J. & Rudolf-Miklau, F. Possibilities and Limitations of Dendrogeomorphic Time-Series Reconstructions on Sites Influenced by Debris Flows and Frequent Snow Avalanche Activity. *Arct. Antarct. Alp. Res.* **43**, 649–658 (2011).
85. Stoffel, M. Magnitude–frequency relationships of debris flows — A case study based on field surveys and tree-ring records. *Geomorphology* **116**, 67–76 (2010).
86. Shroder, J. F. Dendrogeomorphological Analysis of Mass Movement on Table Cliffs Plateau, Utah. *Quat. Res.* **9**, 168–185 (1978).
87. Corona, C. et al. How much of the real avalanche activity can be captured with tree rings? An evaluation of classic dendrogeomorphic approaches and comparison with historical archives. *Cold Reg. Sci. Technol.* **74–75**, 31–42 (2012).
88. Favillier, A. et al. Spatio-temporal maps of past avalanche events derived from tree-ring analysis: A case study in the Zermatt valley (Valais, Switzerland). *Cold Reg. Sci. Technol.* **154**, 9–22 (2018).
89. Bigler, C. & Rigling, A. Precision and accuracy of tree-ring-based death dates of mountain pines in the Swiss National Park. *Trees* **27**, 1703–1712 (2013).
90. Butler, D. R. & Sawyer, C. F. Dendrogeomorphology and high-magnitude snow avalanches: a review and case study. *Nat. Hazards Earth Syst. Sci.* **8**, 303–309 (2008).
91. Schlägl, M., Fuchs, S., Scheidl, C. & Heiser, M. Trends in torrential flooding in the Austrian Alps: A combination of climate change, exposure dynamics, and mitigation measures. *Clim. Risk Manag.* **32**, 100294 (2021).
92. Bollschiweiler, M. & Stoffel, M. Tree rings and debris flows: Recent developments, future directions. *Prog. Phys. Geogr.* **34**, 625–645 (2010).

93. Giorgi, F. et al. Enhanced summer convective rainfall at Alpine high elevations in response to climate warming. *Nat. Geosci.* **9**, 584–589 (2016).
94. Jomelli, V., Brunstein, D., Déqué, M., Vrac, M. & Grancher, D. Impacts of future climatic change (2070–2099) on the potential occurrence of debris flows: a case study in the Massif des Ecrins (French Alps). *Climatic Change* **97**, 171–191 (2009).
95. Jomelli, V., Brunstein, D., Grancher, D. & Pech, P. Is the response of hill slope debris flows to recent climate change univocal? A case study in the Massif des Ecrins (French Alps). *Climatic Change* **85**, 119–137 (2007).
96. Zimmermann, M., Mani, P. & Romang, H. magnitude-frequency aspects of alpine debris flows, <https://doi.org/10.5169/SEALS-168173> (1997).
97. Rickenmann, D. *Methods for the Quantitative Assessment of Channel Processes in Torrents (Steep Streams)* (CRC PRESS, S.L., 2020).

## Acknowledgements

The authors acknowledge support from the research commission of the Swiss National Park (FoK-SNP). They are grateful to the authorities from the Canton of Grisons (*Amt für Wald und Naturgefahren, Region 5 Südbünden*) for granting access to the disaster cadaster and for valuable inputs during fieldwork and analyses. J.Q. benefitted from a China Scholarship Council PhD grant (No 202004910398).

## Author contributions

C.C. and M.S. designed the study with input from all co-authors. J.Q., A.F., F.L., J.A.B.C., J.L.S., S.G., L.F., Y.Z., M.S. and C.C. participated in fieldwork. J.Q. performed tree-ring analyses and first interpretations of data with the help of A.F. F.L. realized sediment supply assessments. C.C., M.S. and J.Q. wrote a first draft of the paper, J.Q., A.F., F.L., J.A.B.C., J.L.S., S.G., L.F., Y.Z., M.S. and C.C. provided comments and revisions.

## Competing interests

The authors declare no competing interests.

## Additional information

**Supplementary information** The online version contains supplementary material available at <https://doi.org/10.1038/s41467-024-53316-z>.

**Correspondence** and requests for materials should be addressed to Jiazhi Qie or Markus Stoffel.

**Peer review information** Nature Communications thanks Tjalling de Haas, Paul Santi and the other, anonymous, reviewer for their contribution to the peer review of this work. A peer review file is available.

**Reprints and permissions information** is available at <http://www.nature.com/reprints>

**Publisher's note** Springer Nature remains neutral with regard to jurisdictional claims in published maps and institutional affiliations.

**Open Access** This article is licensed under a Creative Commons Attribution-NonCommercial-NoDerivatives 4.0 International License, which permits any non-commercial use, sharing, distribution and reproduction in any medium or format, as long as you give appropriate credit to the original author(s) and the source, provide a link to the Creative Commons licence, and indicate if you modified the licensed material. You do not have permission under this licence to share adapted material derived from this article or parts of it. The images or other third party material in this article are included in the article's Creative Commons licence, unless indicated otherwise in a credit line to the material. If material is not included in the article's Creative Commons licence and your intended use is not permitted by statutory regulation or exceeds the permitted use, you will need to obtain permission directly from the copyright holder. To view a copy of this licence, visit <http://creativecommons.org/licenses/by-nc-nd/4.0/>.

© The Author(s) 2024